e-ISSN: 2320-4230, p-ISSN: 2961-6085

Journal of Drug Discovery and Therapeutics

Available Online at www.jddt.in

CODEN: - JDDTBP (Source: - American Chemical Society)

Volume 11, Issue 06: 2023, 1-8

Analyzing the Instabilities of Tokamak Plasma

Hashmi Sayed Taha [*1], Dr. Puranaik Shankar Naik [2]

[1]Research Scholar, Sunrise University, Alwar

[2]Professor, Sunrise University, Alwar

Received: 14-07-2023 / Revised: 13-08-2023 / Accepted: 19-09-2023

Corresponding author: Hashmi Sayed Taha

Conflict of interest: No conflict of interest.

Abstract:

Large-scale fusion reactions may be produced in the tokamak by magnetically confining the fusion fuel at a high enough density and temperature, or in the plasma state. However, turbulence causes high temperature plasma to reach the Scrape-Off Layer (SOL), the outermost layer of the tokamak with open magnetic field lines channeling particles and heat into a specific area of the vacuum vessel. A primary objective of the ITER project is to show a high gain of fusion power in a tokamak. Metallic plasma-facing components in ITER are selected because to their high heat load tolerance and minimal tritium retention. The operation of tokamaks with metallic components confronting the plasma, however, presents challenges for the management of high-Z impurities, as the build-up of heavy impurities, such tungsten (Z=74), in the plasma core results in large radiation losses and weakens the energy confinement. Tungsten (W) transport in ITER's core region ($P < 0.3$), is anticipated to be governed by turbulent and neoclassical processes, which are highly dependent on temperature, rotation patterns, and the primary ion density.

Keywords Tokamak, Plasma, ITER, Electricity

Introduction

Due to the equal amounts of ions and electrons in plasma, it is a conductor of electricity. It is created when the gas's atoms acquire an electrical charge. The word "plasma" has Greek roots that allude to a pliable substance, and its contemporary English meaning is a straight translation. The term plasma was coined by Irving Langmuir in 1928 due to its resemblance to blood plasma, although Sir William Crookes had already seen it in his 'Crookes tube' (Crookes, 1879).

If test estimates are too high or insightful models are too complicated to achieve, then mimicking plasma miracles is a useful strategy to cope with and comprehend genuine cycles. One special kind of model that is utilized to accurately reproduce plasma marvels is the particle in-cell (PIC) model. Because of their predictability, these codes are helpful for creating copies of the electrostatic plasma sheath, for example. The plasma sheath is perhaps one of the most remarkable features of plasma physics. A layer of positive charge builds up at the plasma-divider interface as a result of electrons' quicker transit owing to their lower mass, resulting in the creation of a charged plasma sheath. The concentration of charges causes a potential drop, also known as a sheath potential, which alters the routes followed by charged particles with respect to

the wall that faces the plasma. This non quasineutral zone of the plasma is very tiny (enlargement: a few Debye lengths), but it determines and is determined by the pathways followed by charged particles as they travel to and from the surface, which has significant ramifications for the physics of the whole plasma volume.

Literature Review

Georgios Nicolaou (2018) We are able to recreate the velocity distributions of space plasmas via spacecraft measurements, providing a comprehensive description of the plasma's kinetic state. Space plasmas are often seen in out-of-equilibrium stationary states, which are characterized by kappa distributions. Therefore, for a complete and correct description of these plasmas, factors that regulate these distributions (the temperature and the kappa index) must be specified. In this work, we provide a new and robust method for calculating the temperature and kappa index of plasma distribution functions that are built from counts recorded by conventional electrostatic sensors within a limited energy range. Our approach is applicable to situations when there is either no observation of the plasma's high-energy tail or very little observation of it. We generate pseudo-observations for typical input plasma properties, taking into account the architecture of the Solar Orbiter mission's ion plasma instrument SWA-PAS, in order to validate our approach. Our approach fits the angular spread of the distribution in a small energy range around the core bulk energy, yielding a reliable approximation of the pertinent plasma properties. We juxtapose the results of our methodology with the input parameters that were used to fabricate synthetic data for a designated range of the kappa index and temperature, as well as for a bulk energy characteristic of the solar wind. We also test our technique against observations from Helios 2, examine how Poisson errors affect the counting statistics of the device, and talk about the possible uses and drawbacks of our approach.

Lynn B Wilson (2019) We report a statistical analysis of 15,210 electron velocity distribution function (VDF) fits that the Wind spacecraft detected within ±2 hours following 52 interplanetary (IP) shocks close to 1 au. The series on electron VDFs near IP shocks consists of three parts, this being the second. For reference and baselines in future study, the electron velocity moment statistics for the dense, low-energy core, tenuous, hot halo, and field-aligned beam/strahl are presented in a statistically significant list of values supported by both tabular lists and histograms. The beam/strahl fit findings in the upstream are presently the most thorough effort to parameterize the beam/strahl electron velocity moments in the ambient solar wind, thanks to the enormous statistics in this inquiry. For the core(halo)[beam/strahl] components, the median density, temperature, beta, and temperature anisotropy values of all fit results are,,, and, with subscripts ec (eh)[eb]. Additionally, this study will be used as a baseline and reference for 1 au for missions such as Solar Orbiter and Parker Solar Probe.

Rui Xu (2020) We use self-consistent one-dimensional particle-in-cell simulations to investigate diffusive shock acceleration (DSA) of electrons in nonrelativistic quasi-perpendicular shocks. We discover that high Mach number quasi-perpendicular shocks may effectively accelerate electrons to power-law downstream spectra with slopes compatible with DSA prediction by examining the parameter space of sonic and Alfvénic Mach numbers. At the shock, magnetic mirroring reflects electrons, which cause nonresonant waves to go upstream. Before being injected into DSA, reflected

electrons go through many cycles of shock-drift acceleration while confined between the shock front and upstream waves. Additionally, even in quasi-perpendicular shocks, which ordinarily do not accelerate protons, strong current-driven waves momentarily alter the shock obliquity and produce a little proton pre-acceleration. These findings have applications in the understanding of intracluster medium in galaxy clusters and nonthermal emission in supernova remnants.

Kristopher Klein et.al (2017) Single-point time series derived from linearly unstable, electrostatic numerical simulations are subjected to a newly described approach that establishes a correlation between electric fields and particle velocity distributions. We modify the form of the correlation, which was previously applied to damped electrostatic systems, to include the effects of drifting equilibrium distributions of the kind that cause bump-on-tail and counter-streaming instabilities. The correlation measures the transfer of phase-space energy density between the electric field and plasma distributions. The correlation is perfect for diagnosing dynamics in systems where access to integrated variables, like energy, is not observably possible since it relies on single-point time series. It is shown that the fundamental physical principles governing unstable systems are characterized by the velocity-space structure of the field-particle correlation. In order to eventually apply this correlation to turbulent, magnetized plasmas and ultimately characterize the nature of processes that damp turbulent fluctuations in the solar wind, it will be helpful to employ it in basic systems.

Bea Zenteno-Quinteros et.al (2023) Commonly observed nonthermal properties in electron velocity distributions in the solar wind include temperature anisotropy and field-aligned skewness. Through wave–particle interactions, these properties may serve as a source of free energy to destabilize various electromagnetic wave modes, which might change the plasma state. Prior theoretical works have mostly examined these nonthermal characteristics and self-generated instability separately. Nevertheless, an analysis of the interaction between these two energy sources is required in order to get a more realistic and accurate knowledge of the kinetic processes in the solar wind. In this research we study the excitation of the parallel propagating whistler mode when it is destabilized by electron populations displaying both field-aligned strahl or skewness and temperature anisotropy by means of linear kinetic theory. We use the core-strahlo model as a substitute to explain the electrons in the solar wind. The benefit of this model is that it uses the strahlo population—a single skew-kappa distribution—to reflect the suprathermal characteristics of halo and strahl electrons. Our results demonstrate that this suprathermal population becomes a more potent and effective source of free energy for disrupting the whistler mode when the electron strahlo has an inherent temperature anisotropy. This implies that the anisotropic strahlo is more involved in processes that are influenced by interactions between waves and particles. The current findings also imply that, when evaluating the significance of instabilities caused by the suprathermal population, the contribution of core anisotropy may be safely ignored. This enables a targeted investigation, especially with respect to the control of the solar wind's electron heat flow.

Overview of Tokamak Micro-turbulence

Particle motion and drift velocities in magnetised plasma

Cyclotron motion and guiding centre

A charged particle "s" traveling in an electric E and magnetic B field has the following equation of motion:

$$m_s \frac{d\mathbf{v_s}}{dt} = e_s(\mathbf{E} + \mathbf{v}_s \times \mathbf{B}). \quad \textbf{(1)}$$

where m_s and e_s represent the particle's mass and charge, respectively, "s", v_s is its velocity.

When there is no electric field and a uniform magnetic field pointing in the z-direction, the equation of motion becomes

$$\frac{d\mathbf{v_s}}{dt} = \frac{e_s B}{m_s}(\mathbf{v}_s \times \mathbf{b}), \quad \textbf{(2)}$$

with b = B/B.

When equation 2 is projected onto (x, y, z) coordinates, it produces:

$$\frac{dv_x}{dt} = \omega_{c,s} v_y, \qquad \frac{dv_y}{dt} = -\omega_{c,s} v_x, \qquad \frac{dv_z}{dt} = 0.$$

(3)

A circular orbital motion with an angular frequency around the magnetic field lines is described by the solution to the aforementioned equations ω_c We refer to this motion as Larmor motion. As for the angular frequency $\omega_{c,s}$= e_sB/$m_s$is referred to as angular (cyclotron) frequency. In a magnetic field of B = 5 T, a deuterium's usual cyclotron frequency is around 7.5 MHz.

Further solving equations 3 above via straightforward replacements, variable separation, and the use of $vx = dx/dt \text{ and } vy = dy/dt$, the answer in the x and y directions becomes into:

$$x = -\rho_s \cos(\omega_{c,s} t), \qquad y = \rho_s \sin(\omega_{c,s} t) \quad (4)$$

Where $\rho_s = \frac{m_s v_s}{e_s B}$ is known as the Larmor radius, and the guiding-center is the particle's center of gyration (Larmor motion). Regarding a Deuterium when B = 5 T and $v_\perp = 7 \times 10^5 m/s$, Larmor radius is around 3.5 mm.

Drift of guiding centre

A non-uniform magnetic field's charge-particle dynamics cause the guiding center to wander. We won't go into detail regarding particle paths and these drifts here since you can get that information in any standard textbook on plasma, for example. We only reiterate how the guiding center evolved, as provided by:

$$\frac{d\mathbf{v_G}}{dt} = e(\mathbf{E} + \mathbf{v_G} \times \mathbf{B}) - \mu \nabla \mathbf{B}. \quad (5)$$

with vG how quickly the guiding center is drifting.

Equation 5 may be solved in both parallel and transverse directions to get the guiding center's drift velocities:

The E×B drift velocity resulting from the electric field's presence

$$\mathbf{v}_{\mathbf{E}\times\mathbf{B}} = \frac{\mathbf{E} \times \mathbf{B}}{B^2} \quad (6)$$

The ∇B drift brought on by magnetic field gradients

$$\mathbf{v}_{\nabla B} = \frac{\mu}{e} \frac{\mathbf{b} \times \nabla B}{B} \quad \textbf{(7)}$$

The centrifugal acceleration that occurs when particles follow the magnetic field lines owing to curvature drift caused by the bending of the field lines

$$\mathbf{v}_c = \frac{m v_{\|}^2}{eB} \mathbf{b} \times (\mathbf{b}.\nabla)\mathbf{b} \quad (8)$$

The drift in polarization caused by an electric field that varies over time

$$\mathbf{v}_p = \frac{m}{eB^2} \frac{d\mathbf{E}_\perp}{dt} \quad (9)$$

In an inhomogeneous electric and magnetic field, these drifts control how charged particles evolve.

In magnetized plasmas, the magnetic field resulting from the gyro-motion of every charged particle is directed against the applied external magnetic field; as a result, the plasma is diamagnetic. The existence of pressure gradients causes a collective fluid velocity for all species. Known as the diamagnetic velocity, it is described as

$$\mathbf{v}_{dia} = \frac{\mathbf{B} \times \nabla p}{ZenB^2}. \quad \textbf{(10)}$$

For a single plasma species plus stationary fields, the fluid motion in equilibrium may be expressed as

$$\mathbf{v}_{fluid} = \mathbf{v}_{dia} + \mathbf{v}_E. \quad \textbf{(11)}$$

Kinetic Ballonning Modes (KBMS)

The interplay between the localized regions of unfavorable magnetic curvature and the plasma pressure gradient, which causes the plasma to bulge out in these areas, is the primary cause of the ballooning mode, an electromagnetic instability. One of the most significant instabilities seen in high confinement mode (H-mode) plasma discharges is thought to be the kinetic ballooning mode, which restricts the highest plasma pressure that can be maintained in a magnetic fusion device. Magnetic tension stabilizes because it causes the field lines to bend, and instability cannot occur until a minimum pressure gradient is reached. In toroidal systems, ballooning modes are large toroidal mode number disturbances characterized by long wavelengths parallel to field lines and small wavelengths perpendicular to the magnetic field. The ballooning parameter provides an approximation of the ballooning mode driving force,

$\alpha = -2\mu_0(Rq^2/B^2)p'(r) = \beta q^2(R/L_p)$, with $R, q, B, \beta, p'(r)$ and R/L_p represent the pressure gradient, its radial scale length, the main radius, the safety factor, the toroidal magnetic field, and the plasma beta. Based on this relationship, it seems that the pressure gradient's ballooning mode threshold may become very tiny when the q-value or the plasma β are elevated. The vital importance of α may be computed using the ideal magnetohydrodynamics equations, which are predicated on the premise that disturbances in the parallel electric field E|| vanish. However, E|| may become finite when kinetic effects such trapped particles, collisional effects, wave-particle resonances, magnetic drift, and limited Larmor radius are taken into account. Kinetic ballooning modes (KBM) are ballooning modes that exhibit these kinetic phenomena. The KBM mode may result in cross-field plasma transport and is crucial for the stability and confinement of fusion plasmas. These modes revolve in the direction of the ions' diamagnetic field and are confined to the torus' outboard side.

Note that KBMs generated by wave particle interactions with thermal ions are also called shear Alfvenic ion temperature gradient modes (AITG) in the literature. Nevertheless, it was eventually shown to be an unstable branch that joined the shear Alfven branch with the Beta-induced Alfven Eigenmode (BAE), which is connected to KBM. Nonetheless, the general fish-bone-like dispersion relation (GFLDR-E) indicates that when the BAE and KBM branches are closely connected, the most unstable AITG mode might become destabilized. This happens when the condition $\Omega_{*pi} \equiv (\omega_{*pi}/\omega_{ti}) \sim \sqrt{(7/4+\tau)q}$ is satisfied, where $\omega_{*pi} =$

$(T_i/eB)k_\theta(\nabla \ln n_i)(1+\eta_i)$ core diamagnetic frequency of plasma ions $\eta_i = \nabla \ln T_i/\nabla \ln n_i$, ω_{ti} is the definition of the thermal ion transit frequency $\omega_{ti} = \sqrt{2T_i/m_i}/qR_0$ (T_i is the mass of the ions and their energy-unit temperature) additionally $\tau = T_e/T_i$ Consequently, when the diamagnetic effects predominate, KBM is unstable. $\Omega_{*pi} >> \sqrt{(7/4+\tau)q}$ and BAE when ion compression effects are dominant and BAE in the presence of dominating ion compression effects $\Omega_{*pi} >> \sqrt{(7/4+\tau)q}$ The thermal ion temperature gradient destabilizes these modes when the plasma β is exceeds a certain level. Because of the interaction between the pressure gradient and unfavorable magnetic curvature, the interchange drive term is the source of KBM instability. The threshold in β arises from the fact that at greater β the Alfven speed $V_A = \omega_A qR,$ with ω_A the Alfvén frequency and $V_A = \sqrt{B^2/\mu_0\rho_m}$ The stabilizing magnetic tension falls as the Alfvén velocity, where ρm is the mass density, decreases. Generally, the optimal MHD limit is larger than the β threshold of KBM, $\beta_{crit} < \beta_{crit}^{MHD}$. It has been shown that at higher β values, $\beta_{crit} > \beta_{crit}^{MHD}$, KBM is susceptible to unsteadiness. Here β_{crit} is the critical β the threshold at which unstable Kinetic Ballooning Modes (KBM) occur and β_{crit}^{MHD} is the ideal MHD β limit.

Normalized parallel structure of the electrostatic potential perturbation ($\emptyset$) and vector potential ($A\|\|$) for conventional tokamak characteristics and for unstable modes such as ITG and KBM: $k_\theta\rho_i = 0.4,\ \epsilon = 0.16,\ \hat{s} = 1.0,\ q = 2.0,\ R/L_{TD} = 9.0,$

$R/L_{nD} = 3.0,\ R/L_{Te} = 0.0,\ R/L_{ne} = 3.0,$ Figure 1 shows that, as a function of the parallel coordinate, there are neither collisions nor toroidal rotation or gradient s The perturbed fields $\delta\emptyset$ and $\delta A\|\|$ are normalised as follows: $\phi = \alpha_L \frac{e\delta\phi}{\rho_* T_i}$ and $A_\| = \alpha_L \frac{\delta A_\|}{\rho_*^2 B_{\rm ref} R_0},$ with $\rho_* = \rho_i/R_0$ and α_L an extra normalizing factor that's used to linear simulations $\mathrm{Re}[\phi] = 1$ and $\mathrm{Im}[\phi] = 0$ at the s position where $|\phi|$ is maximum. One poloidal turn corresponds to $\Delta s = 1$.

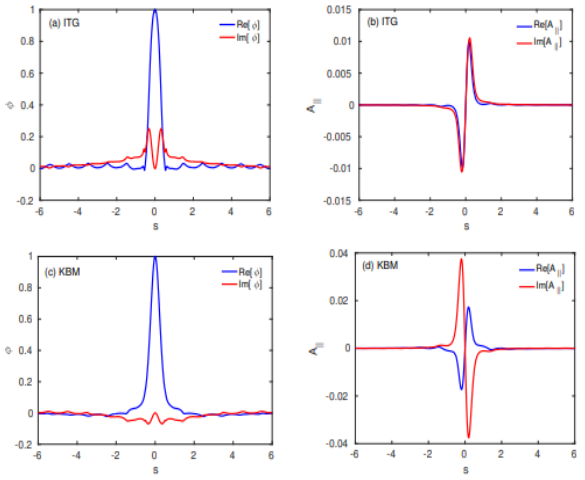

Figure 1: Parallel mode structure of electrostatic potential „ and vector potential A|| for ITG mode (a) and (b), and KBM modes (c) and (d) as a function of parallel coordinate s for standard tokamak parameters given in figure 1.

Ion temperature gradient (ITG) modes become prevalent in beta KBMs over a threshold as the — value rises, as seen in Figure. Compared to their ITG cousin, KBMs occur much more often (Fig. 1(b)).

Figure 1 for a conventional tokamak instance illustrates how both KBM and ITG modes are characterized by an odd parity of parallel vector potential perturbation A|| and an even parity of electrostatic potential perturbation „ along the magnetic field lines.

Conclusion

Tungsten (W) buildup in the center area of the plasma is a major problem that might restrict the capabilities of current and future fusion devices like ITER. Accumulation of tungsten in ITER's core region (p< 0.3) is anticipated to be influenced by turbulent and neoclassical processes. In order to forecast the turbulent W fluxes and background plasma profiles that dictate W neoclassical transport, it is essential to comprehend turbulent transport in this area. Forecasting the region's main transportation p< 0.3 is also crucial for the pace of the fusion reaction. This thesis tests current JET tokamak plasma discharges to determine the suitability of existing reduced transport models for use at ITER. It is considered that the components of the plasma fluid are nano-dust particles, plasma electrons, photoelectrons, and ions, while the micron-sized dust particles act as suspended impurities in the plasma without changing the dynamics of the plasma. It is also thought that the charges on the micron-dusts are derived from their present balance, while the charges on the nano-dusts are fixed.

Reference

1. Nicolaou, Georgios & Livadiotis, George & Owen, Christopher & Verscharen, Daniel & Wicks, Robert. (2018). Determining the Kappa Distributions of Space Plasmas from Observations in a Limited Energy Range. The Astrophysical Journal. 864. 3. 10.3847/1538-4357/aad45d
2. Wilson, Lynn & Chen, Li-Jen & Wang, Shan & Schwartz, Steven & Turner, Drew & Stevens, Michael & Kasper, Justin & Osmane, Adnane & Caprioli, Damiano & Bale, Stuart & Pulupa, Marc & Salem, Chadi & Goodrich, Katherine. (2019). Electron Energy Partition across Interplanetary Shocks. II. Statistics. The Astrophysical Journal Supplement Series. 245. 24. 10.3847/1538-4365/ab5445.
3. Xu, Rui & Spitkovsky, Anatoly & Caprioli, Damiano. (2020). Electron Acceleration in One-dimensional Nonrelativistic Quasi-perpendicular Collisionless Shocks. The Astrophysical Journal. 897. L41. 10.3847/2041-8213/aba11e.
4. Kasper, Justin & Klein, Kristopher. (2019). Strong Preferential Ion Heating is Limited to within the Solar Alfvén Surface. The Astrophysical Journal. 877. L35. 10.3847/2041-8213/ab1de5.
5. Zenteno-Quinteros, Bea & Moya, Pablo & Lazar, Marian & Viñas, Adolfo & Poedts, Stefaan. (2023). Interplay between Anisotropy- and Skewness-driven Whistler Instabilities in the Solar Wind under the Core–Strahlo Model. The Astrophysical Journal. 954. 184. 10.3847/1538-4357/ace973
6. Brinkmann, Ralf. (2011). The plasma-sheath transition in low temperature plasmas: On the existence of a collisionally modified Bohm criterion. Journal of Physics D: Applied Physics. 44. 042002. 10.1088/0022-3727/44/4/042002.
7. Lafleur, T.. (2011). Helicon Wave Propagation in Low Diverging Magnetic Fields.
8. Haruhiko Kohno. (2011). Numerical Analysis of Radio-Frequency Sheath-Plasma Interactions in the Ion Cyclotron Range of Frequencies.
9. Mikellides, Ioannis & Katz, Israel & Hofer, Richard & Goebel, Dan & Grys, Kristi & Mathers, Alex. (2011). Magnetic shielding of the channel walls

in a Hall plasma accelerator. Physics of Plasmas. 18. 033501-033501. 10.1063/1.3551583.

10. Ahedo, Eduardo & Merino, Mario. (2009). Two-Dimensional Plasma Acceleration in a Divergent Magnetic Nozzle. 10.2514/6.2009-5361.
11. Arefiev, Alex & Breizman, Boris. (2009). Collisionless plasma expansion into vacuum: Two new twists on an old problem. Physics of Plasmas. 16. 055707-055707. 10.1063/1.3118625.
12. Ahedo, Eduardo. (2009). Parametric analysis of a magnetized cylindrical plasma. Physics of Plasmas. 16. 10.1063/1.3262529.
13. Onishi, Tatsuo & Berthelier, J.-J & Forest, Jene & Marchand, Richard. (2009). Effects on plasma and electric field measurements induced by spacecraft-plasma interaction.
14. Zehua, Guo & Tang, Xianzhu. (2012). Parallel transport of long mean-free-path plasmas along open magnetic field lines: Plasma profile variation. Physics of Plasmas. 19. 10.1063/1.4747167.
15. Fruchtman, Amnon & Takahashi, Kazunori & Boswell, R.. (2012). A magnetic nozzle calculation of the force on a plasma. Physics of Plasmas. 19. 10.1063/1.3691650.